

Supporting Information

Interface Engineering of NiV-LDH@FeOOH Heterostructures as High-Performance Electrocatalysts for Oxygen Evolution Reaction in Alkaline Conditions

Weiwei Bao^a, Lei Xiao^a, Junjun Zhang^{b,*}, Zhifeng Deng^a, Chunming Yang^c, Taotao Ai^{a,*}, Xueling Wei^a

^aNational & Local Joint Engineering Laboratory for Slag Comprehensive Utilization and Environmental Technology, School of Material Science and Engineering, Shaanxi University of Technology, Hanzhong 723000, Shaanxi, China

^bSchool of Materials Science and Chemical Engineering, Xi'an Technological University, Xi'an, Shaanxi 710021, China

^cShaanxi Key Laboratory of Chemical Reaction Engineering, College of Chemistry & Chemical Engineering, Yan'an University, Yan'an, Shaanxi, 716000, China

***Corresponding Author**

Junjun Zhang, E-mail: zhangjunjun@xatu.edu.cn

Taotao Ai, E-mail: aitaotao0116@126.com

List of Contents

1. Experimental Section:

- 1.1. Materials
- 1.2. Synthesis of NiV-LDH/NF sample
- 1.3. Synthesis of NiV-LDH@FeOOH/NF sample
- 1.4. Preparation of RuO₂ electrode on Ni foam
- 1.5. General characterizations
- 1.6. Electrochemical Test

2. Supplementary Figures:

- Figure S1.** The SEM images of bare NF (a) with low-magnification (b, c) with high-magnification.
- Figure S2.** The SEM images of (a) NiV-LDH/NF and (b) NiV-LDH@FeOOH/NF electrodes.
- Figure S3.** The EDS spectrum of NiV-LDH@FeOOH/NF electrode.
- Figure S4.** The XRD patterns of (a) NiV-LDH@FeOOH/NF hybrid electrode and NiV-LDH powder (b) and FeOOH powder (c).
- Figure S5.** The photo of three electrode test system.
- Figure S6.** CV curve for NiV-LDH/NF (a) and NiV-LDH@FeOOH/NF (b) hybrid electrode.
- Figure S7.** (a) The iR-corrected linear sweep voltammograms and (b) the EIS of the FeOOH/NF and NiV-LDH@FeOOH/NF hybrid electrode.
- Figure S8.** The EIS of NiV-LDH@FeOOH/NF electrode under different test conditions.
- Figure S9.** The EIS of the bare Ni foam, NiV-LDH/NF, NiV-LDH@FeOOH/NF and commercialized RuO₂ electrodes measured in O₂ saturated 1.0 M KOH solution (pH = 14).
- Figure S10.** The direct hydrophilic and hydrophobic test.
- Figure S11.** (a) The iR-corrected linear sweep voltammograms, (b) The EIS of the NiV-LDH@FeOOH/NF electrodes with different synthesis times measured in O₂ saturated 1.0 M KOH solution (pH = 14).
- Figure S12.** The multi-potential steps of NiV-LDH@FeOOH/NF electrode.
- Figure S13.** (a) XPS Spectrum and (b) high-resolution Ni 2p XPS spectrum of NiV-LDH@FeOOH/NF hybrid electrode before and after OER test.
- Figure S14.** STEM image and corresponding EDX elemental mapping images for NiV-LDH@FeOOH/NF hybrid electrode after OER test.
- Figure S15.** SEM image for NiV-LDH@FeOOH/NF hybrid electrode after OER test.
- Figure S16.** High-resolution (a) Ni 2p (b) V 2p and (c) O 1s XPS spectra of NiV-LDH/NF and NiV-LDH powder samples.
- ### 3. Supplementary Tables:
- Table S1.** Comparison of the performance NiV-LDH@FeOOH/NF with other reference samples
- Table S2.** Comparison of the OER activity of NiV-LDH@FeOOH/NF with other reported non-noble metal-based electrocatalysts in basic media (1 M KOH).
- Table S3.** Comparison of the EIS parameter of NiV-LDH@FeOOH/NF with other reference samples.
- ### 4. Notes and references

1. Experimental Section

1.1 Materials

Nickel nitrate hexahydrate ($\text{Ni}(\text{NO}_3)_2 \cdot 6\text{H}_2\text{O}$), vanadium trichloride (VCl_3), urea ($\text{CO}(\text{NH}_2)_2$), sodium nitrate (NaNO_3), hexahydrate ferric chloride ($\text{FeCl}_3 \cdot 6\text{H}_2\text{O}$), ruthenium dioxide (RuO_2), and Nafion (5 wt%) were purchased from Shinopharm Chemical Reagent Co., Ltd. Milli-Q ultrapure water was used for all experiments. Nickel foam (NF) were used as the substrate. All chemicals were used as received without further purification.

1.2. Synthesis of NiV-LDH/NF sample

The one-step hydrothermal method was employed to prepare the NiV-LDH/NF. In a typical synthesis process, a piece of Ni foam ($1 \times 4 \text{ cm}^2$) was treated in HCl solution (2.0 M) under the ultrasonication for 15 min to remove the surface oxide layer, followed by sonicating in ethanol and deionized water for 15 min, respectively. Then, 0.175 g $\text{Ni}(\text{NO}_3)_2 \cdot 6\text{H}_2\text{O}$, 0.076 g VCl_3 , and 0.24 g urea were dissolved in 30 mL deionized water and stirred for 30 min to form homogeneous solution. Afterwards, the precursor solution was transferred into a Teflon-lined stainless steel autoclave (50 mL). Subsequently, the as-cleaned Ni foam ($1 \times 4 \text{ cm}^2$) was submerged into the above solution. The autoclave was heated to 130 °C for 12 h in an electric oven. After cooling to room temperature, the as-prepared NiV-LDH/NF was washed with deionized water and ethanol for several times, and then dried in an oven at 60 °C, 12h.

1.3 Synthesis of NiV-LDH@FeOOH/NF sample

For preparing NiV-LDH@FeOOH/NF electrode, 2.547g NaNO_3 and 1.217g $\text{FeCl}_3 \cdot 6\text{H}_2\text{O}$ was dissolved in 30 mL deionized water and kept at 100 °C for 8 min. Then, the as-prepared NiV-LDH/NF was immersed into the pre-heated solution within a certain amount of time. The as-prepared NiV-LDH@FeOOH/NF electrode was washed with ethanol for several times, and then further dried in an oven at 60 °C, 2h. The average mass loading of catalyst on Ni foam is about $3 \text{ mg} \cdot \text{cm}^{-2}$.

1.4 Preparation of RuO_2 electrode on Ni foam

A total of 3 mg RuO₂ powder was dispersed in 200 μL deionized water, 200 μL of ethanol and 15 μL of 15wt% Nafion solution through ultrasound for 30 min to form a uniform suspension. Powder ink was loaded onto as-cleaned Ni foam (1 × 1 cm²), followed with the dry in air at room temperature. The average mass loading of RuO₂ on Ni foam is about 3 mg · cm⁻².

1.5 General characterizations

The morphology of as-prepared catalysts was characterized by field-emission scanning electron microscope (FESEM, JSM-7610F, 10 kV), transmission electron microscope (TEM) (JSM-7610F, 10 kV). The surface characteristics of the samples were investigated using X-ray photoelectron spectroscopy (XPS) measurements (Kratos Axis Ultra DLD spectro meter.)

1.6 Electrochemical Test

All the electrochemical tests were proceeded in a standard three-electrode system by a CHI660E electrochemical station (CH Instruments, Inc., Shanghai) at room temperature. For detail, NiV-LDH/NF, NiV-LDH@FeOOH/NF and bare Ni foam were directly used as the working electrode, a graphite carbon rod was used as counter electrode and a mercury oxide electrode (Hg/HgO) was used as reference electrode. All electrochemical measurements were carried out in 1 M KOH solution. The measured potentials were transformed to reversible hydrogen electrode (RHE) according to the equation: $E_{\text{RHE}} = E_{\text{Hg/HgO}} + 0.059 \times \text{pH} + 0.098$. The OER measurements were recorded by linear sweep voltammetry (LSV) at a scan rate of 5 mV s⁻¹. All polarization curves were corrected by iR losses. The plots of electrochemical impedance spectroscopy (EIS) were measured with 5 mV amplitude in a frequency of 0.01 Hz ~ 100 kHz.

2. Supplementary Figures:

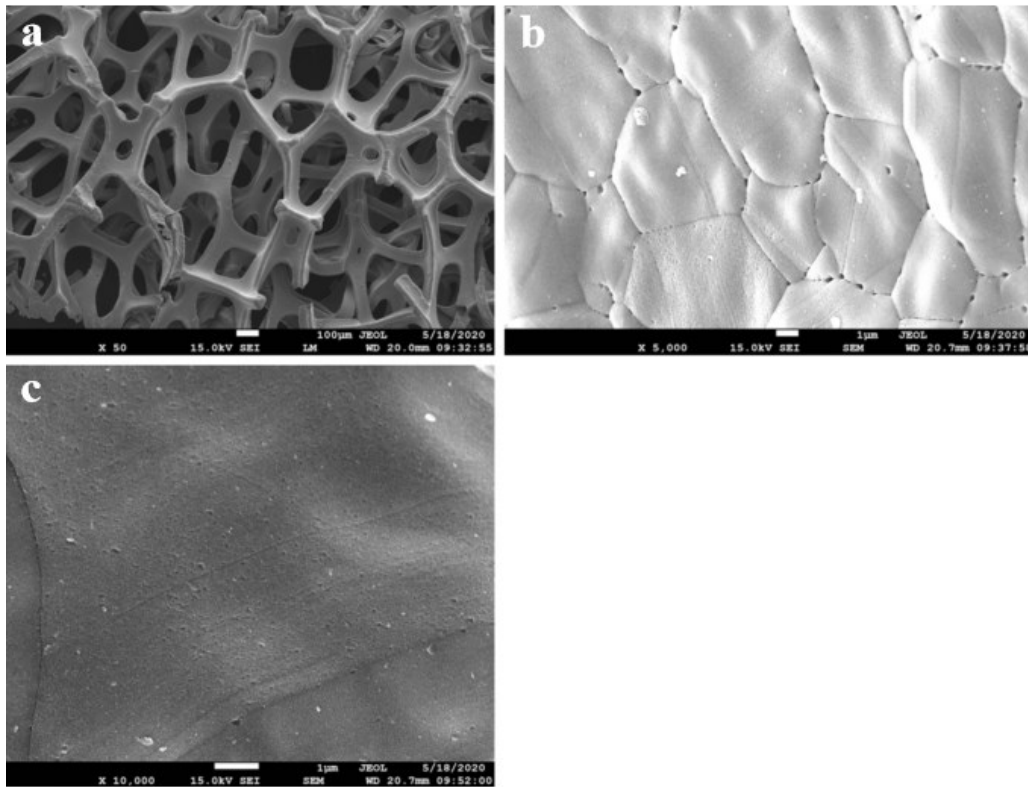


Figure S1. The SEM images of bare NF (a) with low-magnification (b, c) with high-magnification.

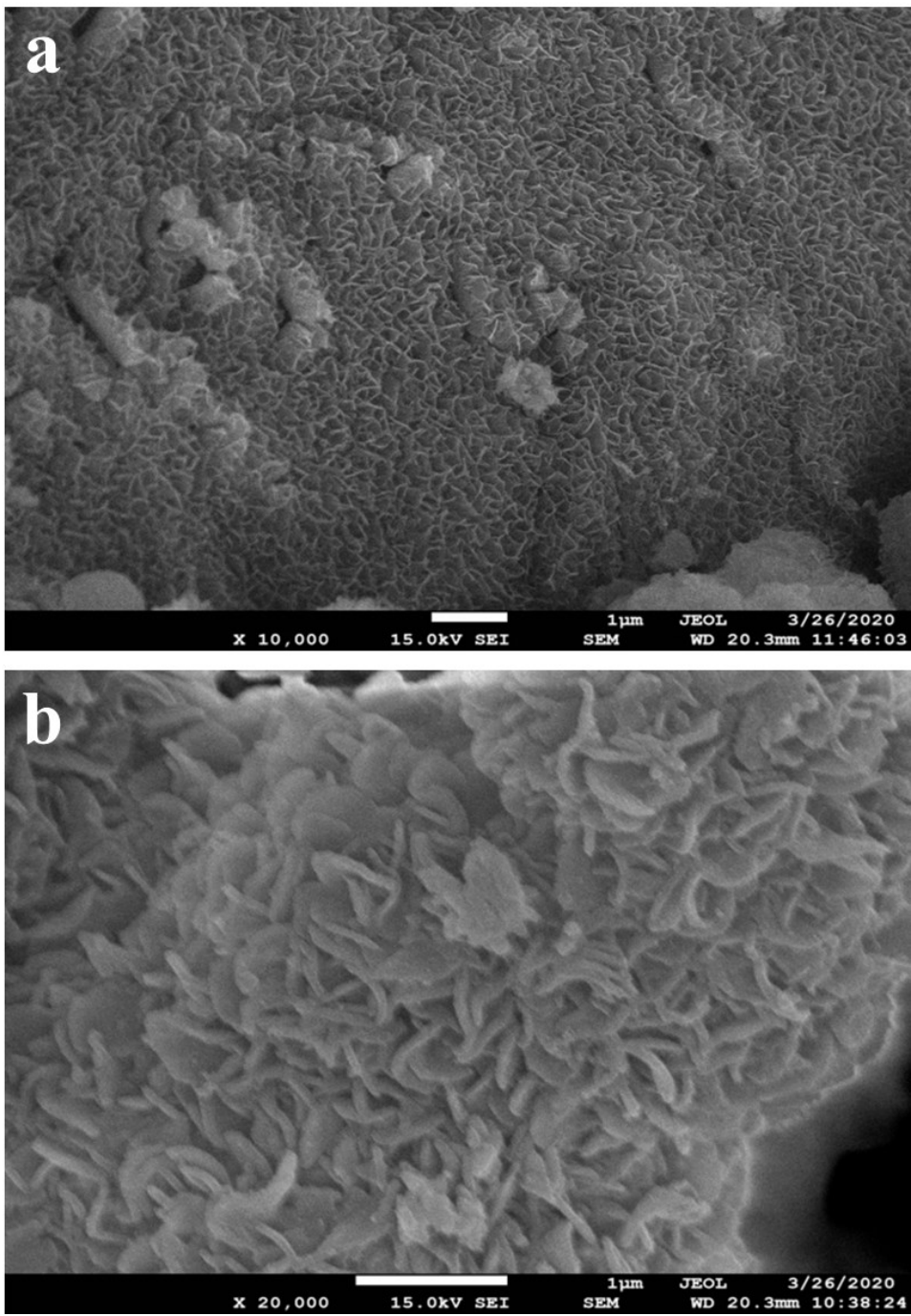


Figure S2. The SEM images of (a) NiV-LDH/NF and (b) NiV-LDH@FeOOH/NF electrodes.

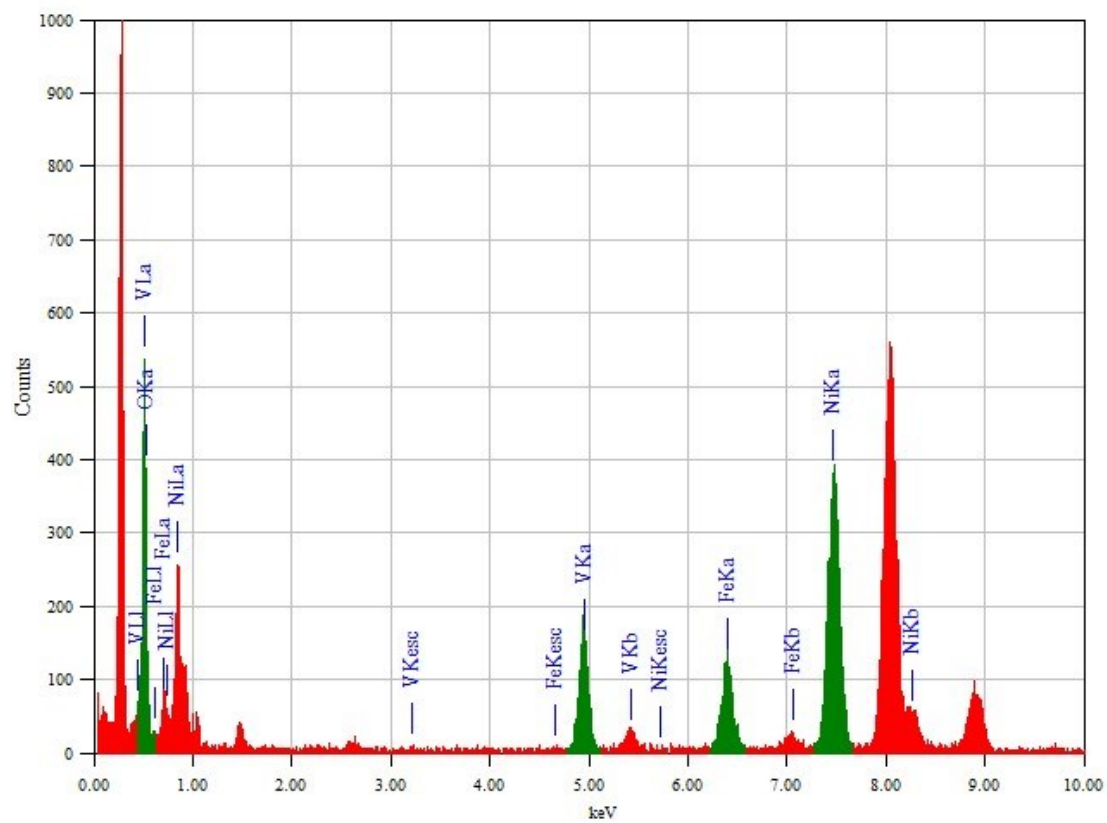


Figure S3. The EDS spectrum of NiV-LDH@FeOOH/NF electrode.

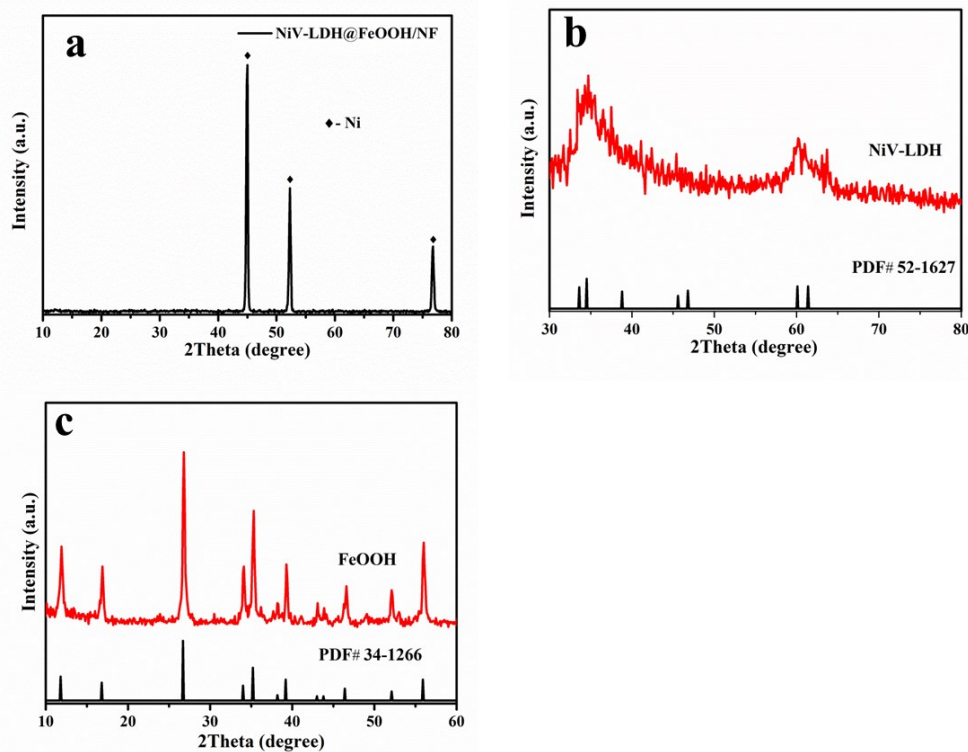


Figure S4. The XRD patterns of (a) NiV-LDH@FeOOH/NF hybrid electrode and NiV-LDH powder (b) and FeOOH powder (c).

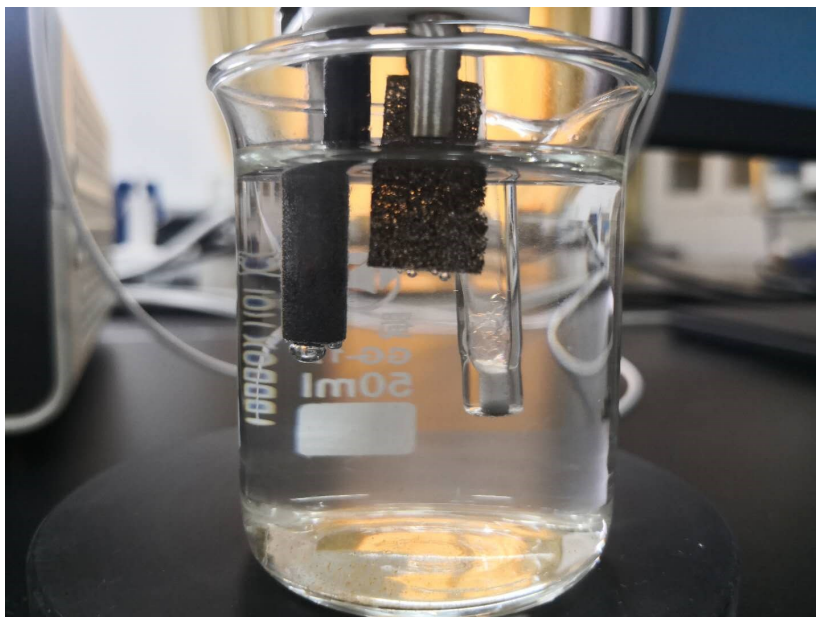


Figure S5. The photo of three electrode test system. NiV-LDH@FeOOH/NF was directly used as the working electrode, a graphite carbon rod was used as counter electrode and a mercury oxide electrode (Hg/HgO) was used as reference electrode.

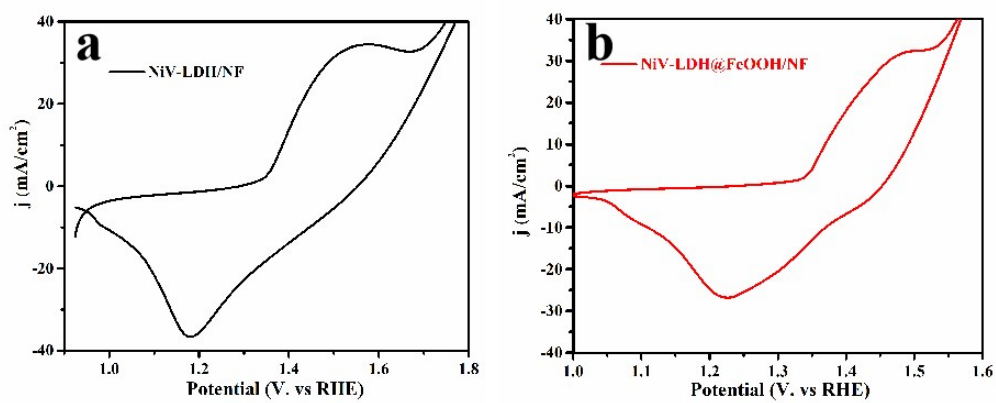


Figure S6. CV curve for NiV-LDH/NF (a) and NiV-LDH@FeOOH/NF (b) hybrid electrode.

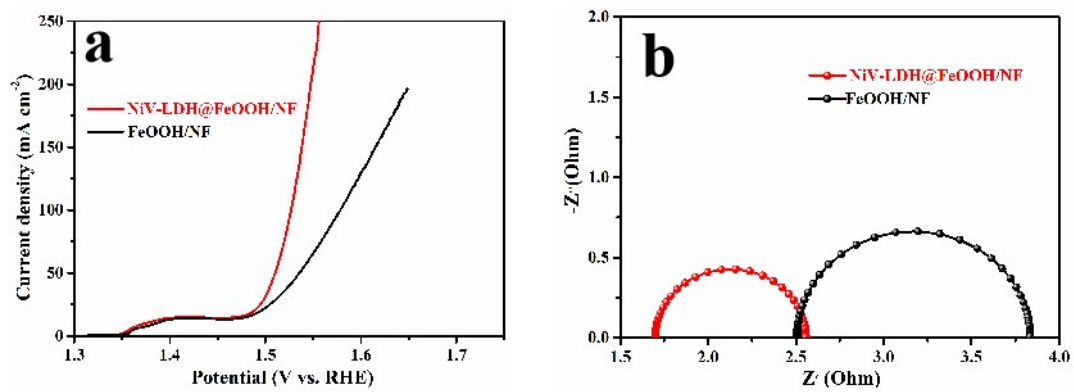


Figure S7. (a) The iR-corrected linear sweep voltammograms and (b) the EIS of the FeOOH/NF and NiV-LDH@FeOOH/NF hybrid electrode.

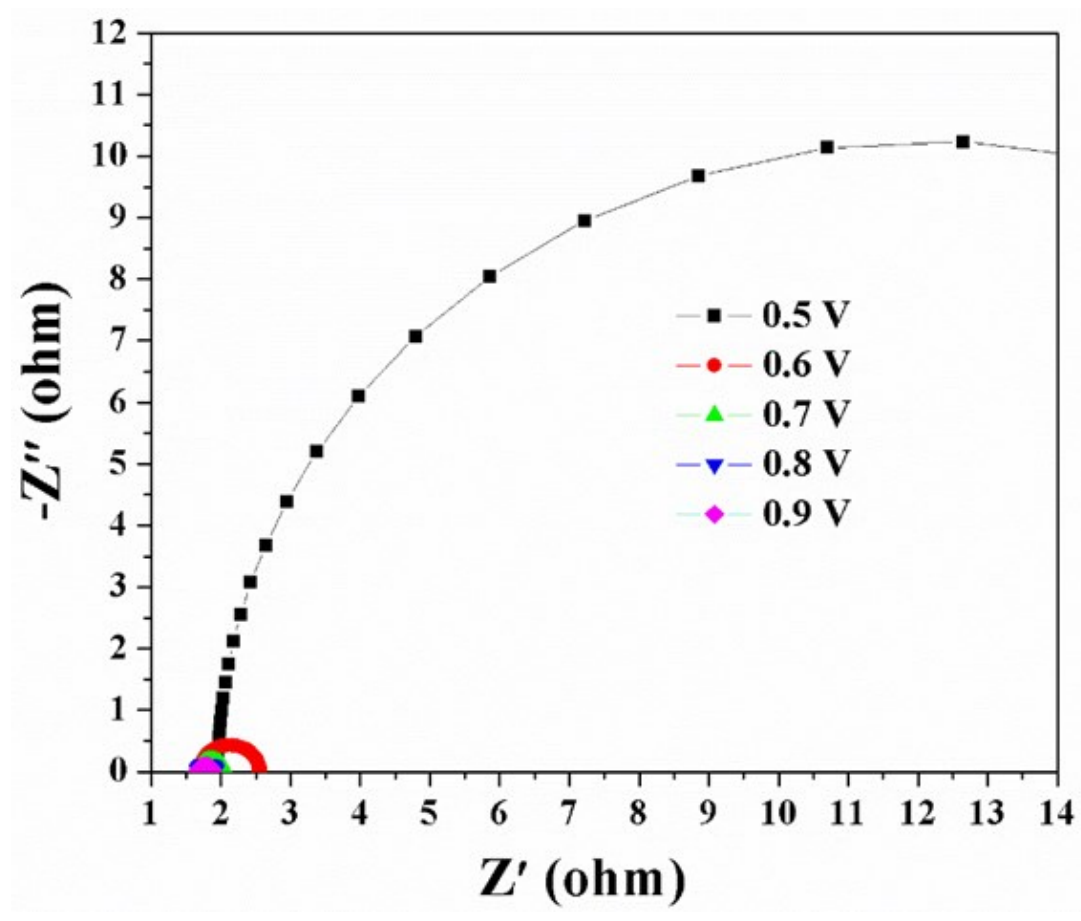


Figure S8. The EIS of NiV-LDH@FeOOH/NF electrode under different test conditions.

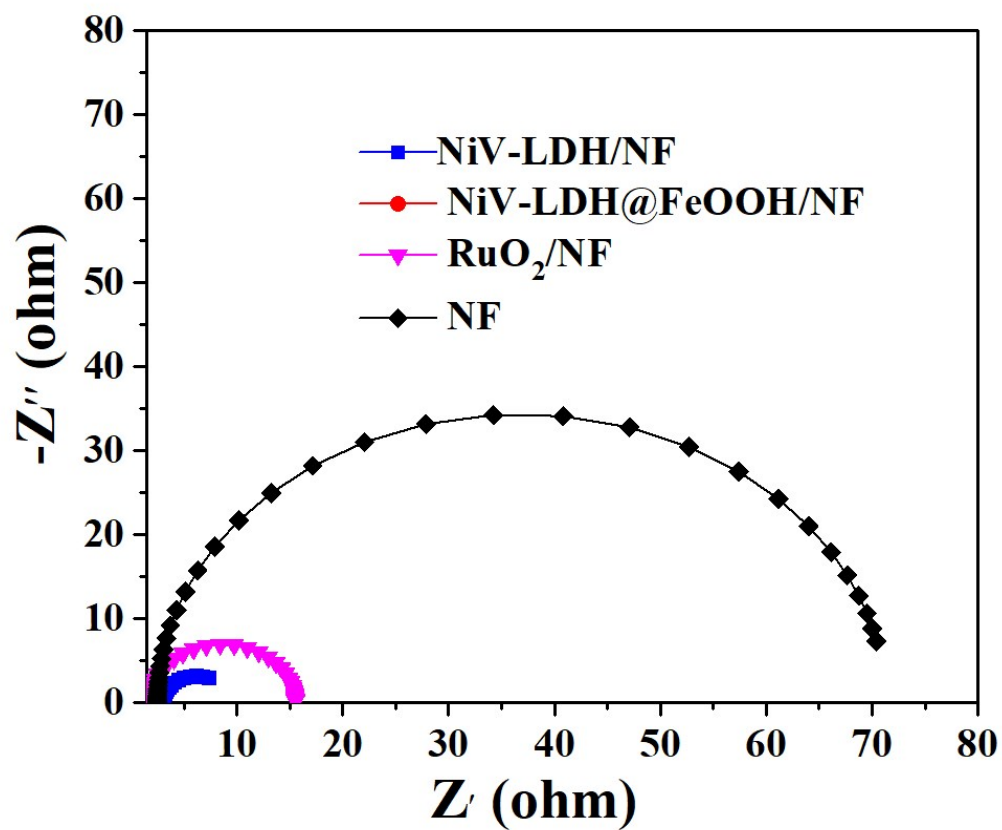


Figure S9. The EIS of the bare Ni foam, NiV-LDH/NF, NiV-LDH@FeOOH/NF and commercialized RuO₂ electrodes measured in O₂ saturated 1.0 M KOH solution (pH = 14).

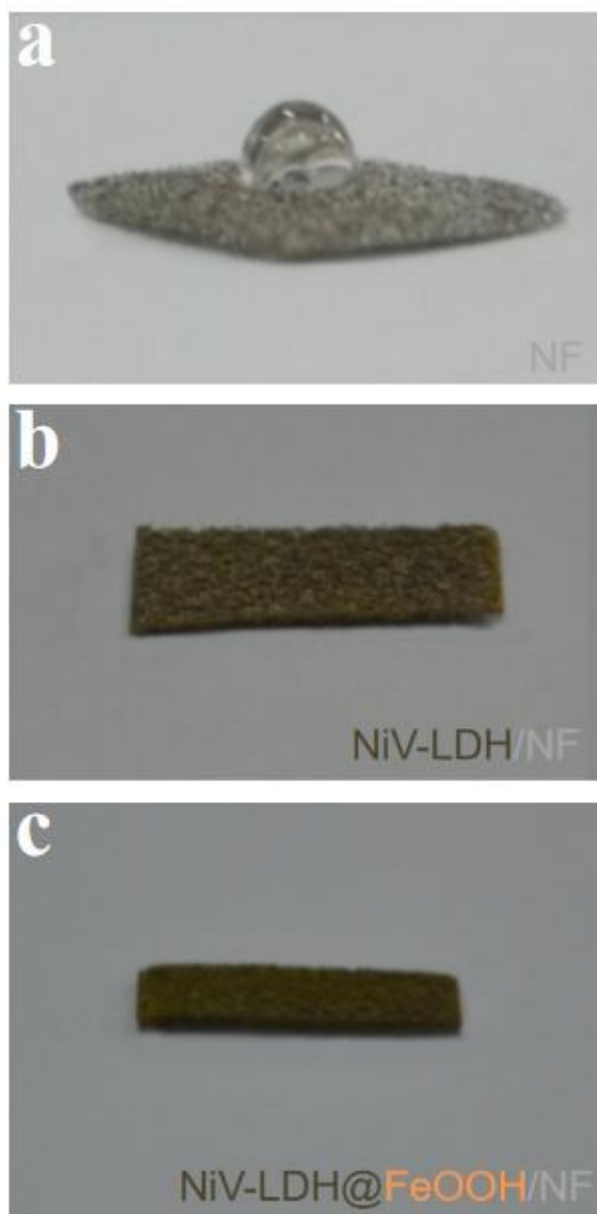


Figure S10. The direct hydrophilic and hydrophobic test.

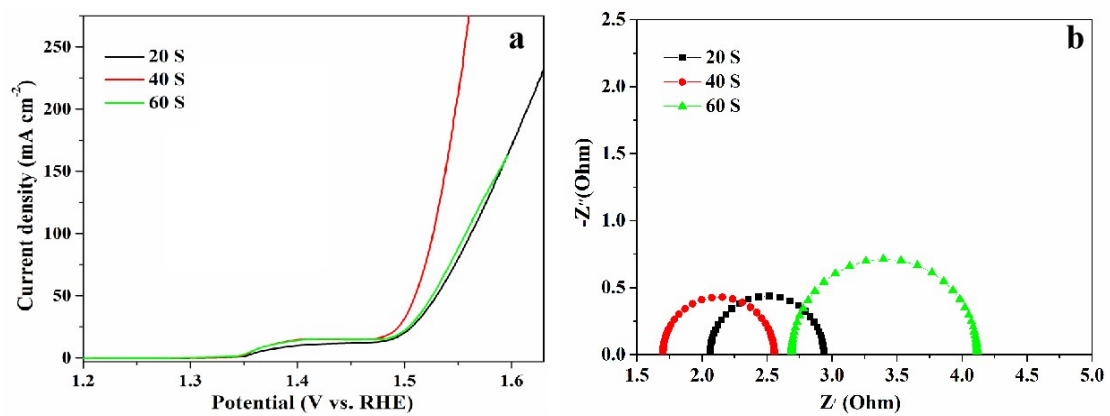


Figure S11. (a) The iR -corrected linear sweep voltammograms, (b) The EIS of the NiV-LDH@FeOOH/NF electrodes with different synthesis times measured in O_2 saturated 1.0 M KOH solution (pH = 14).

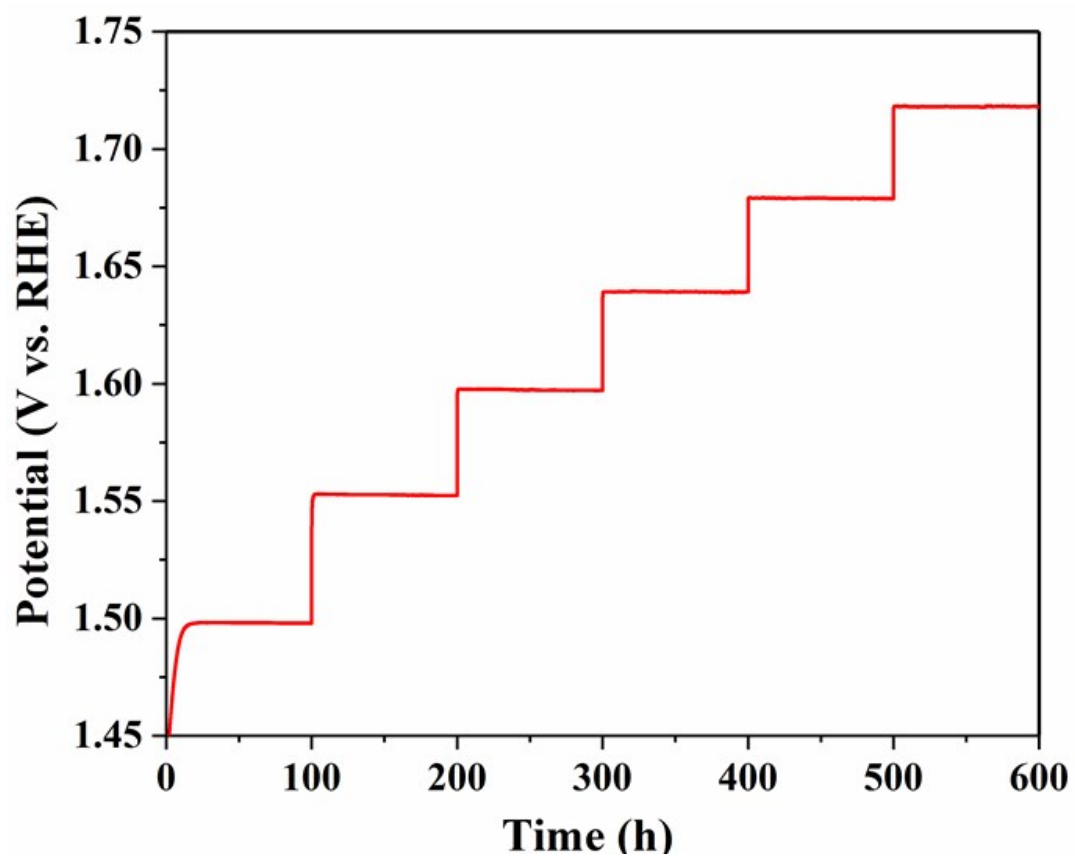


Figure S12. The multi-potential steps of NiV-LDH@FeOOH/NF electrodes.

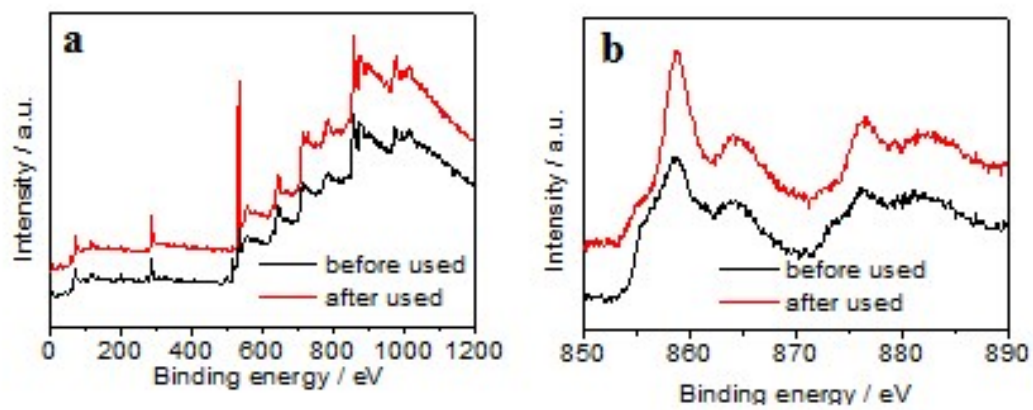


Figure S13. (a) XPS Spectrum and (b) high-resolution Ni 2p XPS spectrum of NiV-LDH@FeOOH/NF hybrid electrode before and after OER test.

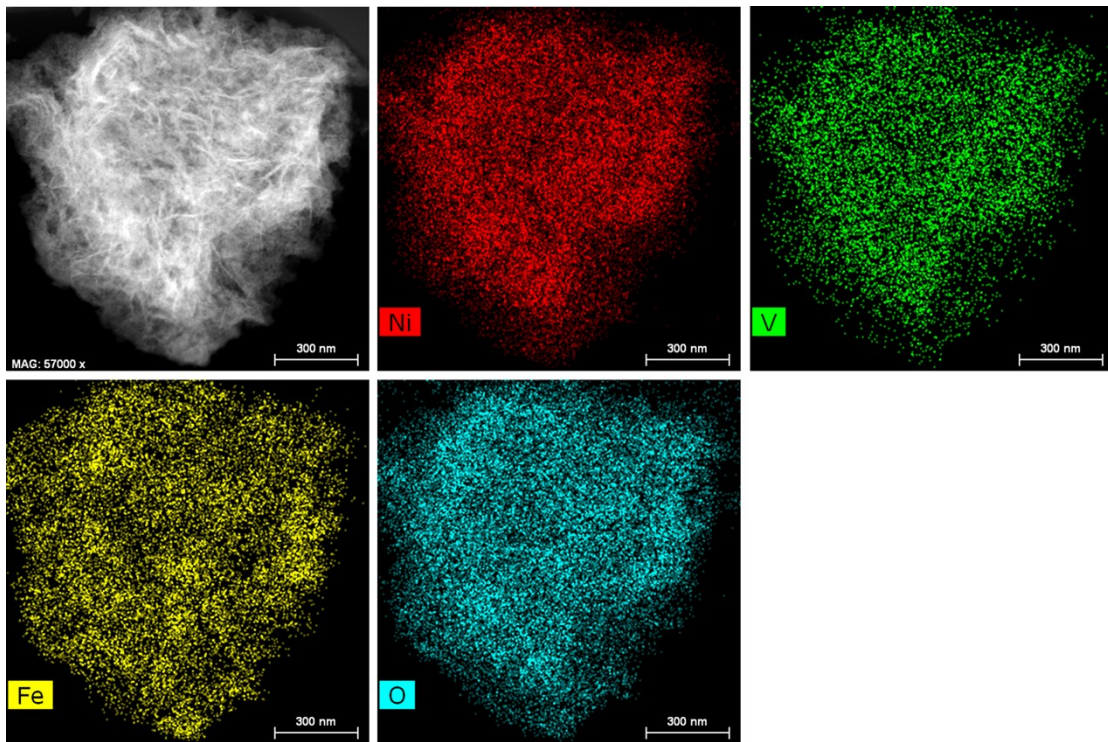


Figure S14. STEM image and corresponding EDX elemental mapping images for NiV-LDH@FeOOH/NF hybrid electrode after OER test.

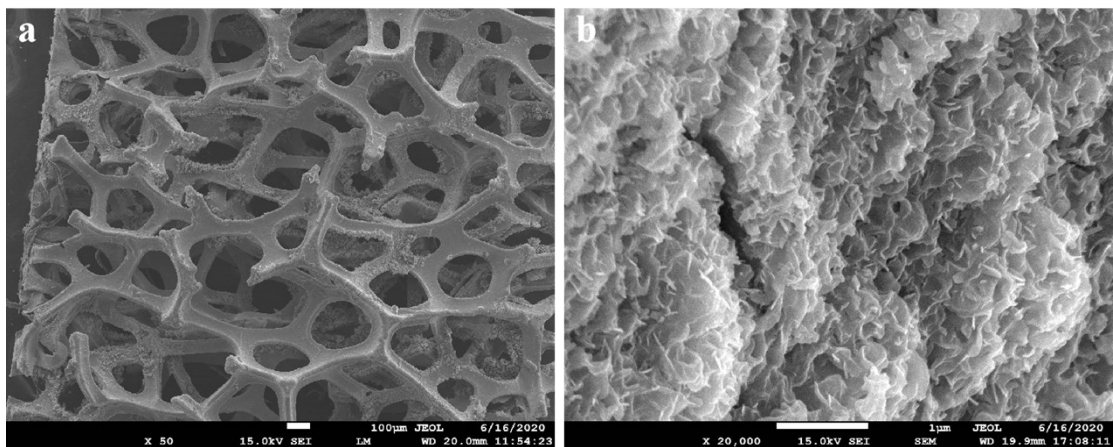


Figure S15. SEM image for NiV-LDH@FeOOH/NF hybrid electrode after OER test.

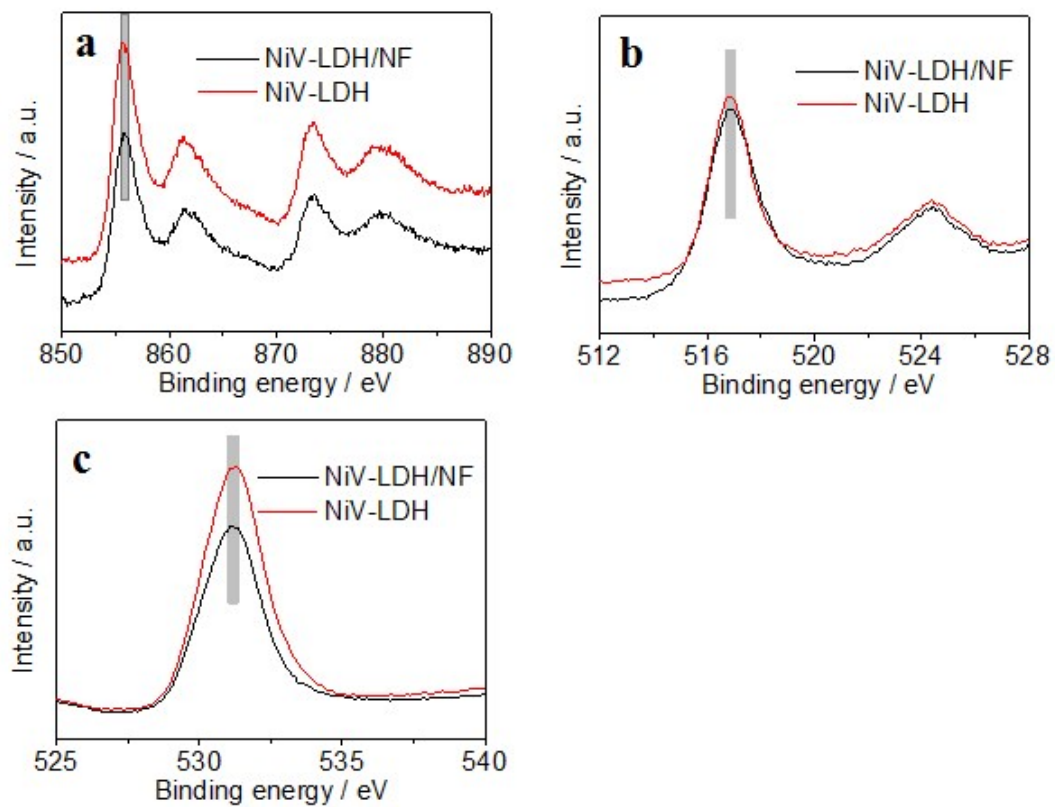


Figure S16. High-resolution (a) Ni 2p (b) V 2p and (c) O 1s XPS spectra of NiV-LDH/NF and NiV-LDH powder samples.

Supplementary Table S1 Comparison of the performance NiV-LDH@FeOOH/NF with other reference samples.

Samples	Onset potential / V vs. RHE	Over potential at j=100mA cm⁻² (V vs. RHE)
NiV-LDH@FeOOH/NF	1.49	297
NiV-LDH/NF	1.58	472
RuO₂	1.55	467
Ni foam	1.60	528

Supplementary Table S2 Comparison of the OER activity of NiV-LDH@FeOOH/NF with other reported non-noble metal-based electrocatalysts in basic media (1 M KOH).

Catalysts	Loading/ mg cm ⁻²	Current density (mA/cm ²)	Overpotential (mV)	Reference
NiV-LDH@FeOOH/NF	3.0	100	297	This work
(Co-Pi)	0.285	100	420	1. Chem. Commun., 2020,56, 4575-4578
NiCo ₂ O ₄	0.27	10	320	2. J. Mater. Chem. A, 2020,8, 8554-8565
NiCoP-rGO	0.15	10	270	3. Adv. Funct. Mater. 2016, 26, 6785-6796
NiFe LDH/graphene	2	100	325	4. Adv. Mater. 2017, 29, 1700017-1700024.
Ni-Fe-OH@Ni ₃ S ₂ /NF	22.2	100	300	5. Adv. Mater. 2017, 29, 1700404-17004010.
FeOOH/Co/FeOOH	0.5	100	308	6. Angew. Chem. Int. Ed. 2016, 55, 3694-3698.
W _{0.5} Co _{0.4} Fe _{0.1} /NF	-----	100	310	7. Angew. Chem. Int. Ed. 2017, 56, 4502-4506.
NiCo LDH/CFP	0.8	100	370	8. Carbon 2016, 110, 1-7.
NiFe LDH/NF	-----	100	460	9. Science 2014, 345, 1593-1596.
Ni(OH) ₂ /Ni ₃ S ₂ /NF	-----	100	490	10. J. Mater. Chem. A. 2018, 6, 6938-6946.
NiCo ₂ S ₄ NW/NF	-----	100	470	11. Adv. Funct. Mater. 2016, 26, 4661-4672.
Co ₁ Mn ₁ CH/NF	5.6	100	349	12. J. Am. Chem. Soc. 2017, 139, 8320-8328.
Hollow NiCo ₂ O ₄	1	100	360	13. Angew. Chem. Int. Ed. 2016, 55, 6290-6294.
Ni ₃ S ₂ @NiV-LDH	0.71	100	320	14. Nanoscale, 2019, 11, 8855-8863.
Co-CoO _x /CN	2.1	50	360	15. J. Am. Chem. Soc. 2015, 137, 2688-2694.
NiFe-LDH/NiCo ₂ O ₄ /NF	4.9	50	290	16. ACS Appl. Mater. Inter. 2017, 9, 1488-1495
Au-Ir	0.02	10	245	17. Nature Communications, 2020, DOI:10.1038/s41467-020-15391-w
NiFeMn-LDH	0.102	10	310	18. Chem. Commun., 2016, 52, 908-911.
Ni ₃ FeAl _x -LDH/NF	0.5	20	304	19. Nano Energy 2017, 35, 350-357.
Co ₂ Mo ₃ O ₈	0.14	10	241	20. Angew. Chem. Int. Ed. 2020, DOI: 10.1002/anie.202004533

Supplementary Table S3 Comparison of the EIS parameter of NiV-LDH@FeOOH/NF with other reference samples.

Samples	R_{ct}/ ohm	R_Ω/ ohm
NiV-LDH@FeOOH/NF	0.85	1.699
NiV-LDH/NF	4.3	2.966
RuO₂	13.8	1.696
Ni foam	67.9	2.469

4. Notes and references

1. Jindi Qi, Junfeng Xie, Zimeng Wei, Shanshan Lou, Pin Hao, Fengcai Leia, Bo Tang. Modulation of crystal water in cobalt phosphate for promoted water oxidation. *Chem. Commun.*, 2020, 56, 4575-4578.
2. José Béjar, Lorena Álvarez-Contreras, Janet Ledesma-García, Noé Arjon, Luis Gerardo Arriaga. An advanced three-dimensionally ordered macroporous NiCo₂O₄ spinel as a bifunctional electrocatalyst for rechargeable Zn–air batteries. *J. Mater. Chem. A*, 2020,8, 8554-8565.
3. Jiayuan Li, Ming Yan, Xuemei Zhou, Zheng-Qing Huang, Zhaoming Xia, Chun-Ran Chang, Yuanyuan Ma, Yongquan Qu. Mechanistic Insights on Ternary Ni_{2-x}Co_xP for Hydrogen Evolution and Their Hybrids with Graphene as Highly Efficient and Robust Catalysts for Overall Water Splitting. *Adv. Funct. Mater.* 2016, 26, 6785-6796.
4. Yi Jia, Longzhou Zhang, Guoping Gao, Hua Chen, Bei Wang, Jizhi Zhou, Mun Teng Soo, Min Hong, Xuecheng Yan, Guangren Qian, Jin Zou, Aijun Du, Xiangdong Yao. A Heterostructure Coupling of Exfoliated Ni-Fe Hydroxide Nanosheet and Defective Graphene as a Bifunctional Electrocatalyst for Overall Water Splitting. *Adv. Mater.* 2017, 29, 1700017-1700024.
5. Xu Zou, Yipu Liu, Guo-Dong Li, Yuanyuan Wu, Da-Peng Liu, Wang Li, Hai-Wen Li, Dejun Wang, Yu Zhang, Xiaoxin Zou. Ultrafast Formation of Amorphous Bimetallic Hydroxide Films on 3D Conductive Sulfide Nanoarrays for Large-Current-Density Oxygen Evolution Electrocatalysis. *Adv. Mater.* 2017, 29, 1700404-1700410.
6. Jin-Xian Feng, Han Xu, Yu-Tao Dong, Sheng-Hua Ye, Ye-Xiang Tong, Gao-Ren Li. FeOOH/Co/FeOOH Hybrid Nanotube Arrays as High-Performance Electrocatalysts for the Oxygen Evolution Reaction. *Angew.Chem. Int. Ed.* 2016, 55, 3694-3698.
7. Yecan Pi, Qi Shao, Pengtang Wang, Fan Lv, Prof. Shaojun Guo, Prof. Jun Guo, Xiaoqing Huang. Trimetallic Oxyhydroxide Coraloids for Efficient Oxygen Evolution Electrocatalysis. *Angew. Chem. Int. Ed.* 2017, 56, 4502-4506.
8. Chang Yu, Zhibin Liu, Xiaotong Han, Huawei Huang, Changtai Zhao, Juan Yang, Jieshan Qiu. NiCo-layered double hydroxides vertically assembled on carbon fiber papers as binder-free high-active electrocatalysts for water oxidation. *Carbon* 2016, 110, 1-7.
9. Jingshan Luo, Jeong-Hyeok Im, Matthew T. Mayer, Marcel Schreier, Mohammad Khaja Nazeeruddin, Nam-Gyu Park, S. David Tilley, Hong Jin Fan, Michael Grätzel. Water photolysis at 12.3% efficiency via perovskite photovoltaics and Earth-abundant catalysts. *Science*, 2014, 345, 1593-1596.
10. Xiaoqiang Dua, Zhi Yanga, Yu Lia, Yaqiong Gong, Min Zhao. Controlled synthesis of Ni(OH)₂/Ni₃S₂ hybrid nanosheet arrays as highly active and stable electrocatalysts for water splitting. *J. Mater. Chem. A*. 2018, 6, 6938-6946.
11. Arumugam Sivanantham, Pandian Ganesan, Sangaraju Shanmugam. Hierarchical NiCo₂S₄ Nanowire Arrays

Supported on Ni Foam: An Efficient and Durable Bifunctional Electrocatalyst for Oxygen and Hydrogen Evolution Reactions. *Adv. Funct. Mater.* 2016, 26, 4661-4672.

12. Tang Tang, Wen-Jie Jiang, Shuai Niu, Ning Liu, Hao Luo, Yu-Yun Chen, Shi-Feng Jin, Feng Gao, Li-Jun Wan, Jin-Song Hu. Electronic and Morphological Dual Modulation of Cobalt Carbonate Hydroxides by Mn Doping toward Highly Efficient and Stable Bifunctional Electrocatalysts for Overall Water Splitting. *J. Am. Chem. Soc.* 2017, 139, 8320-8328.

13. Xuehui Gao, Hongxiu Zhang, Quanguo Li, Xuegong Yu, Zhanglian Hong, Xingwang Zhang, Chengdu Liang, Zhan Lin. Hierarchical NiCo₂O₄ Hollow Microcuboids as Bifunctional Electrocatalysts for Overall Water-Splitting. *Angew. Chem. Int. Ed.* 2016, 55, 6290-6294.

14. Qianqian Liu, Jianfeng Huang, Yajuan Zhao, Liyun Cao, Kang Li, Ning Zhang, Dan Yang, Li Feng, Liangliang Feng. Tuning the coupling interface of ultrathin Ni₃S₂@NiV-LDH heterogeneous nanosheet electrocatalysts for improved overall water splitting. *Nanoscale*, 2019, 11, 8855-8863.

15. Haiyan Jin, Jing Wang, Diefeng Su, Zhongzhe Wei, Zhenfeng Pang, Yong Wang. In situ Cobalt-Cobalt Oxide/N-Doped Carbon Hybrids As Superior Bifunctional Electrocatalysts for Hydrogen and Oxygen Evolution. *J. Am. Chem. Soc.* 2015, 137, 2688-2694.

16. Zhiqiang Wang, Sha Zeng, Weihong Liu, Xingwang Wang, Qingwen Li, Zhigang Zhao, Fengxia Geng. Coupling Molecularly Ultrathin Sheets of NiFe-Layered Double Hydroxide on NiCo₂O₄ Nanowire Arrays for Highly Efficient Overall Water-Splitting Activity. *ACS Appl. Mater. Inter.* 2017, 9, 1488-1495.

17. Ran Du, Jinying Wang, Ying Wang, René Hübner, Xuelin Fan, Irena Senkowska, Yue Hu, Stefan Kaskel, Alexander Eychmüller. Unveiling reductant chemistry in fabricating noble metal aerogels for superior oxygen evolution and ethanol oxidation. *Nat Commun* 11, 1590 (2020). <https://doi.org/10.1038/s41467-020-15391-w>.

18. Zhiyi Lu, Li Qian, Yang Tian, Yaping Li, Xiaoming Sun and Xue Duan, Ternary NiFeMn layered double hydroxides as highly-efficient oxygen evolution catalysts, *Chem. Commun.*, 2016, 52, 908-911.

19. Haixia Liu, Yanrong Wang, Xinyao Lu, Yi Hua, Guoyin Zhu, Renpeng Chen, Lianbo Ma, Hongfei Zhu, Zuoxiu Tie, Jie Liu. The effects of Al substitution and partial dissolution on ultrathin NiFeAl ternary layered double hydroxide nanosheets for oxygen evolution reaction in alkaline solution. *Nano Energy* 2017, 35, 350-357.

20. Zhao-Qing Liu, Ting Ouyang, Xiao-Tong Wang, Xiu-Qiong Mai, An-Na Chen, Zi-Yuan Tang. Coupling Magnetic Single-Crystal Co₂Mo₃O₈ with Ultrathin Nitrogen-Rich Carbon Layer for Oxygen Evolution Reaction. *Angew. Chem. Int. Ed.* 2020, DOI: 10.1002/anie.202004533.